

# Nonlinear Creep Deformation of Polycarbonate at High Stress Level: Experimental Investigation and Finite Element Modeling

Daiki Ikeshima, Akihiro Matsuzaki, Takumi Nagakura, Kanako Emori, and Akio Yonezu

(Submitted August 1, 2018; in revised form November 5, 2018; published online February 19, 2019)

It is well known that polycarbonate (PC) undergoes time-dependent deformation (i.e., creep deformation), and nonlinear creep deformation is often experienced at high stress level. Using the time–temperature–stress superposition principle (TTSSP), we obtain a new master curve, which covers higher stress level, and successfully establish a new modeling method of creep deformation of PC. First, to investigate the effect of applied stress level on the creep compliance (i.e., stress-dependent nonlinear creep deformation), this study conducted various creep tests with eight different stress levels. We found that the creep compliance curve strongly depended on the applied stress level; in particular, a higher stress level induced a larger difference in creep compliance. According to the TTSSP, the creep compliance curve at each stress level shifts with the creep time (i.e., stress reduced time). When we appropriately selected the stress reduced time, we obtained the master curve of creep compliance, which is unified with respect to various applied stresses. However, we found that the stress-shifted factor is not compliant with the previous TTSSP, especially in the higher stress regime. Therefore, this regime was also considered to obtain a new master curve that can cover a wide range of stress levels. Finally, our established creep model (master curve and stress shift factor) was introduced into FEM, and then this numerical model was verified by comparison with experimental data. Our model may be useful for predicting the creep deformation of PC subjected to a wide range of applied stresses.

**Keywords** finite element method, nonlinear creep deformation behavior, polycarbonate, stress shift factor, time–stress superposition principle

## 1. Introduction

Engineering polymer materials have been widely used in a variety of engineering fields. In particular, polycarbonate (PC) has been used as a structural material in a wide range of industrial applications such as the automotive and aircraft components industry due to their excellent impact strength, good processability, transparency and high heat distortion temperature (Ref 1–3). Most engineering polymer materials undergo deformation with time dependency due to the intrinsic viscosity of the involved materials. This is strongly influenced by temperature (Ref 4–7), humidity (Ref 5), physical aging (Ref 8, 9), damage (Ref 10, 11), pressure, solvent concentration (Ref 12, 13) and applied strain and stress levels (Ref 14–18). Thus, the mechanism of time-dependent deformation behavior is complicated, resulting in difficulty in establishing a creep deformation model; nevertheless, modeling the time-dependent deformation behavior of structural polymer materials is important.

It is well known that the combined Maxwell model, Voigt–Kelvin model and Boltzmann superposition principle can be used to predict the deformation behavior, in particular the linear viscoelastic behavior of polymer materials. For example, Kichenin et al. (Ref 19) used the linear viscoelastic–plastic model for their numerical model and successfully simulated the deformation behavior of polyethylene. Lu et al. (Ref 20) and Seltzer et al. (Ref 21) developed methods to determine the linear viscoelastic–plastic response using the indentation method and inverse analytical solution. However, these methods are generally acceptable for linear viscoelastic materials. In other words, the relationship between applied stress and time-dependent deformation behavior is a linear relationship because nonlinear viscoelastic properties are infinitesimally small and are therefore negligible. However, polymer materials often exhibit nonlinear viscoelastic properties with longer testing time, when applied stress is larger, or both.

Therefore, much research in modeling nonlinear viscoelastic behavior has been done; in particular, attention has been paid to creep deformation behavior. Sakai et al. (Ref 4) conducted the creep testing of PC at high temperature with short-term testing time to examine linear and nonlinear creep deformation. They discussed the feasibility of creep compliance parameters, including various factors such as temperature, fiber volume fraction and heat treatment conditions. Jazouli et al. (Ref 18) conducted uniaxial tensile creep testing of PC at a large applied stress with a short testing time and investigated the applied stress effect on the creep deformation behavior. Luo et al. (Ref 22) conducted uniaxial tensile creep testing of polymethyl methacrylate at various temperatures and applied stress levels to investigate the effects of applied stress and temperature on the creep deformation behavior. They used the time–tempera-

Daiki Ikeshima, Akihiro Matsuzaki, Takumi Nagakura, Kanako Emori, and Akio Yonezu, Department of Precision Mechanics, Chuo University, 1-13-27 Kasuga, Bunkyo, Tokyo 112-8551, Japan. Contact e-mail: yonezu@mech.chuo-u.ac.jp.

ture–stress superposition principle (TTSSP) (Ref 17, 18, 22–25) for polymer creep testing, in which the creep compliance curve at different temperatures or stress levels can be shifted along the time scale by using a master curve at a reference temperature or stress level. They successfully obtained a master curve for creep compliance, which can be acceptable for a wide range of applied stress levels. Therefore, nonlinear creep deformation under different applied stresses can be predicted (Ref 18). However, their creep tests were conducted for about 1 h, which may be too short. In this case, the feasibility of TTSSP may still be unclear. In order to examine industrial applications further, a longer period may be required. Moreover, the principle of nonlinear creep must be introduced into numerical computation (such as the finite element method, FEM), since FEM computation effectively simulates mechanical deformation behavior under various mechanical loadings.

This study aims to establish a numerical model for the nonlinear creep deformation of PC. Our model covers large applied stresses and relatively long testing times. First, uniaxial tensile creep tests were conducted at eight different stress levels to investigate creep compliances with respect to the applied stress level. To eliminate the stress dependency of creep compliance, a master curve for creep compliance using a reference stress level and appropriate shift factor was obtained. The shift factor of the master curve was theoretically investigated on the basis of free volume theory. We thus established a master curve for creep compliance, which can cover various stress levels. Finally, the established master curve was verified using tension tests on a circular hole sample; here, the tensile stress was developed with a gradient because of the stress concentration near the hole. Such a test was also conducted numerically by using FEM, which included our master curve. We thus established a computational FEM model for the nonlinear creep deformation of PC. This may be useful for other loading cases including stress gradient conditions and multiaxial stress states.

## 2. Theoretical Background

As described in section 1, TTSSP has been reported upon in previous studies (Ref 17, 18, 23–25). It was then used in this study to establish a FEM model for nonlinear creep deformation. TTSSP was established because large stress levels and high temperatures accelerate creep deformation (Ref 17, 18, 23–25). This theory is fundamentally based on the free volume theory based on the Doolittle equation (Ref 26). According to the free volume theory, the viscosity of materials ( $\eta$ ) can be calculated by using the Doolittle equation:

$$\eta = A \exp(B/f) \quad (\text{Eq 1})$$

where  $A$  and  $B$  are material constants and  $f$  is the free volume fraction, which is the occupied free volume in the entire polymeric material.

The principle assumes that the thermal and stress-induced increment in the free volume fraction is linear. The free volume fraction can be expressed as follows:

$$f = f_0 + \alpha_T(T - T_0) + \alpha_\sigma(\sigma - \sigma_0) \quad (\text{Eq 2})$$

where  $\alpha_T$  and  $\alpha_\sigma$  are the coefficients of thermal and stress-induced expansion, respectively, and  $f_0$  is the free volume fraction at a given stress ( $\sigma = \sigma_0$ ) and temperature ( $T = T_0$ ).

At constant stress, i.e.,  $\sigma = \sigma_0$ , we define the temperature shift factor,  $\Phi_T = \tau/\tau_0 = \eta/\eta_0$ , where  $\eta_0$  and  $\tau_0$  are, respectively, the material viscosity and relaxation time at reference temperature  $T_0$  ( $\eta$  and  $\tau$  are, respectively, the material viscosity and relaxation time at a given temperature  $T$ ). There exists a temperature shift factor  $\Phi_T$  that can satisfy the following relationship:

$$\eta(T, \sigma) = \eta(T_0, \sigma)\phi_T \quad (\text{Eq 3})$$

By using Eq 1 and 2, we therefore obtain:

$$\log \phi_T = -\frac{B}{2.303f_0} \left( \frac{T - T_0}{\frac{f_0}{\alpha_T} + T - T_0} \right) = -\frac{C_1(T - T_0)}{C_3 + (T - T_0)} \quad (\text{Eq 4})$$

Equation 4 indicates the WLF (Williams–Landel–Ferry) equation (Ref 5).

Similar to Eq 4, the stress shift factor  $\Phi_\sigma$  when the temperature is constant ( $T = T_0$ ) is defined as below:

$$\log \phi_\sigma = -\frac{B}{2.303f_0} \left( \frac{\sigma - \sigma_0}{\frac{f_0}{\alpha_\sigma} + \sigma - \sigma_0} \right) = -\frac{C_1(\sigma - \sigma_0)}{C_2 + (\sigma - \sigma_0)} \quad (\text{Eq 5})$$

At a nonconstant applied stress ( $\sigma \neq \sigma_0$ ) and nonconstant temperature ( $T \neq T_0$ ), the stress–temperature shift factor  $\Phi_{T\sigma}$  is calculated by using Eq 4 and 5:

$$\log \phi_{T\sigma} = -C_1 \left[ \frac{C_3(\sigma - \sigma_0) + C_2(T - T_0)}{C_2C_3 + C_3(\sigma - \sigma_0) + C_3(T - T_0)} \right] \quad (\text{Eq 6})$$

This study focuses on the effect of stress level on the creep deformation behavior of PC (i.e., nonlinear creep deformation with stress dependency). Using  $\Phi_\sigma$  as calculated by Eq 5, we can therefore describe the creep compliance  $J(t)$  ( $J(t)$  = creep strain normalized by applied constant stress) of the nonlinear creep deformation via the stress-induced reduced time  $t/\Phi_\sigma$ :

$$J(\sigma, t) = J(\sigma_0, t/\phi_\sigma) \quad (\text{Eq 7})$$

In this study, the effect of temperature on the creep deformation is not discussed.

## 3. Experimental Setup of Creep Tests

The material used in this study was PC board (PC-1600, C. I. Takiron Corp.), which is commercially available. This study conducted uniaxial tensile tests for two types of specimen: a smooth specimen and a circular hole specimen. The smooth specimen was dumbbell-shaped; for this, a gage area of 60 mm length  $\times$  10 mm width  $\times$  2 mm thickness was used. We reported that this type of test yielded the elastoplastic properties of the material (Young's modulus and yield strength) (Ref 27). The circular hole specimen was rectangular in shape (130 mm length  $\times$  36 mm width  $\times$  2 mm thickness) with one circular hole at the center having a diameter of 16 mm. In this study, annealing process was conducted for 3 h at 150 °C.

Tensile creep testing was carried out by using a ball-screw-type universal testing machine (AG-1, Shimadzu Corp.) at room temperature (21 °C) and for 10<sup>5</sup> s. Before creep testing, uniaxial tensile testing was conducted under a displacement

control of 3 mm/min ( $8.3 \times 10^{-4} \text{ s}^{-1}$  strain rate) until the desired applied stress was reached. To measure the creep strain, an extensometer with camera image data was used with no contact. The mark tracking technique was used to obtain the uniaxial strain. In the specimen, two markers were placed along the gage length of the specimen. The distance of the two markers was 60 mm for the smooth specimen and 120 mm for the circular hole specimen. In order to investigate the effect of the applied stress level on the creep compliance (nonlinear creep), this study conducted tests at stresses ranging from 12.4 to 49.8 MPa (12.4, 18.6, 24.9, 31.1, 37.3, 40.4, 43.5 and 49.8 MPa). Each test was conducted at least twice to check the reproducibility.

For the circular hole specimen, tensile creep testing was carried out using the same experimental setup. Before creep testing, uniaxial tensile testing was conducted under a displacement control at 3 mm/min ( $8.3 \times 10^{-4} \text{ s}^{-1}$  strain rate) until the desired loading was achieved (namely, a force of 750 N) and constant loading was applied for  $4 \times 10^4 \text{ s}$ . In this case, the net normal stress (without the hole area) was 10.5 MPa. If a specimen has a circular hole in center, the stress  $\sigma_{\max}$  at the edge of circular hole can be calculated by Howland analytical solution (Ref 28) as follows:

$$\sigma_{\max} = K_t \frac{P}{t(H-d)} \quad (\text{Eq 8})$$

where  $K_t$  is stress concentration factor,  $P$  is tensile loading,  $t$  is thickness of the specimen,  $H$  is width of the specimen, and  $d$  is diameter of the circular hole. In this solution,  $K_t$  is calculated by Eq 9.

$$K_t = \left(1 - \frac{d}{H}\right) \times \left(0.284 + \frac{2}{1 - \frac{d}{H}} - 0.6 \left(1 - \frac{d}{H}\right) + 1.32 \left(1 - \frac{d}{H}\right)^2\right) \quad (\text{Eq 9})$$

Given that the values of  $d$  and  $H$  are 16 mm and 36 mm, respectively,  $K_t$  is 2.2 and  $\sigma_{\max}$  is 41.2 MPa. Therefore, we expected that a large stress gradient develops in the sample. We then examined the stress dependency of creep compliance (i.e., nonlinear creep deformation behavior).

## 4. Results and Discussion

### 4.1 Tensile Creep Deformation

Figure 1 shows the creep strain as a function of creep time at eight different applied stresses. We found that the strain increases with testing time, with the strain becoming larger at larger applied stresses.

According to the linear viscoelastic theory, creep deformation can be evaluated by using the creep compliance  $J(t)$  as follows:

$$\varepsilon(t) = \int_0^t J(t-\tau) \frac{d\sigma}{d\tau} d\tau \quad (\text{Eq 10})$$

where  $\varepsilon(t)$  is the creep strain, which is a function of time  $t$  and  $\tau$ , while  $\sigma$  is the applied stress (Ref 29). Note that the applied stress was constant in this study (see section 3). Using Eq 10,

we obtained the creep compliance curves as shown in Fig. 2. It suggests that the creep compliance curves are strongly dependent on the applied stress level, suggesting that PC exhibits nonlinear creep deformation.

According to TTSSP, creep compliance curves can be unified by using reduced time (horizontally shifted in Fig. 2), even if the creep compliance curves vary with the applied stress. As shown in Fig. 2, the creep compliance curves of the stress level at 12 MPa and 18 MPa did not coincide with each other. Thus, the curve for 12 MPa was selected at the reference stress  $\sigma_0$  in this study. By shifting the horizontal axis in Fig. 2, we obtained the master curve for creep compliance as shown in Fig. 3. In other words, we obtained a unified master curve and the relationship between  $\Phi_\sigma$  and the stress difference in Eq 5 when we appropriately determined  $t/\Phi_\sigma$  of Eq 7, as shown in Fig. 4. In order to use the numerical model (FEM), the master curve in Fig. 3 was fitted with the following equation:

$$J(t) = J_0 \cdot \exp(K \cdot \log(t/\phi_\sigma)) \quad (\text{Eq 11})$$

where  $J_0$  and  $K$  are material constants. This function is referred to as the creep model for polyvinylidene fluoride (Ref 30), which may be widely available. By fitting the master curve with Eq 9, we can obtain the values of  $J_0$  ( $1.87 \times 10^{-6} \text{ 1/MPa}$ ) and  $K$  (0.53), for which the correlation coefficient  $R^2$  shows a value of 0.97.

As shown for the shift factor  $\Phi_\sigma$  in Fig. 4, we found that the stress level below  $\sigma = 37 \text{ MPa}$  ( $\sigma - \sigma_0 = 24.9 \text{ MPa}$ ) is in good agreement with Eq 5. At stresses larger than 37 MPa, the stress shift factors deviated from Eq 5. Therefore, the trend of stress shift factor in this study was divided into two regimes. Regime I could be fitted with Eq 5, and regime II was observed to deviate from Eq 5. Fitting of regime I with Eq 5 yielded

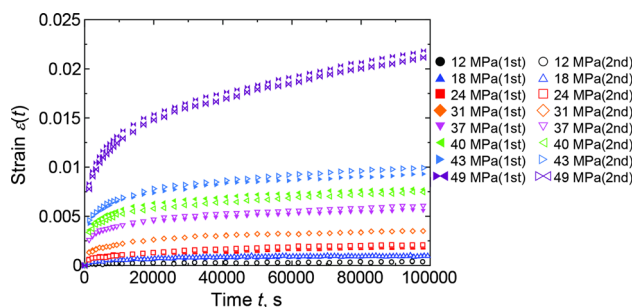


Fig. 1 Creep strain curves as a function of creep time at eight different applied stress levels

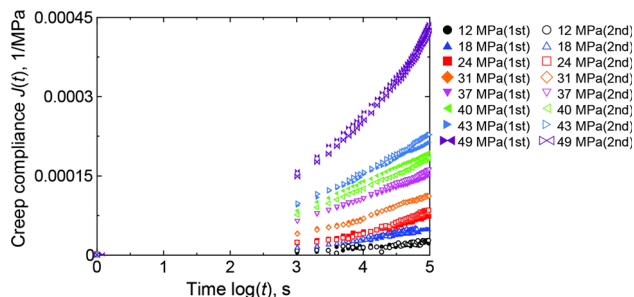
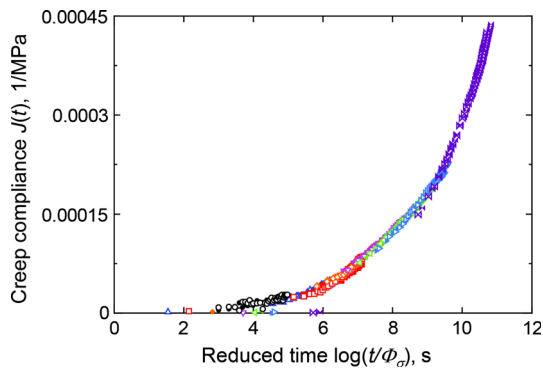
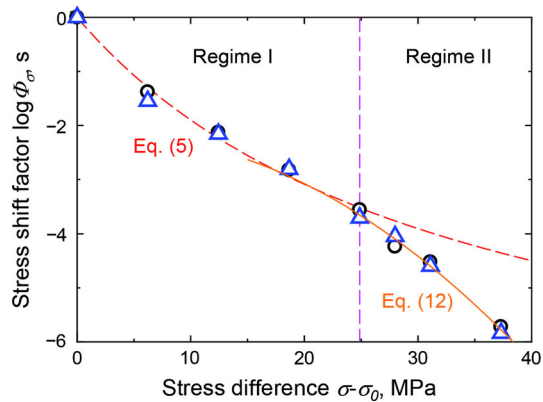


Fig. 2 Creep compliance curves as a function of creep time at eight different applied stress levels



**Fig. 3** Master curve for the creep compliance at a reference stress of 12 MPa and room temperature



**Fig. 4** Variation of stress shift factor as a function of stress difference from  $\sigma_0 = 12$  MPa and room temperature; open circles and open triangles represent the first and second experiments, respectively

$C_1 = -8.3$  and  $C_2 = 33.5$  MPa. Comparison with previous studies (Ref 5, 18) revealed that the value of  $C_1$  is in agreement with those previously obtained. Subsequently, regime II was fitted with the following equation with a second-order polynomial function:

$$\log \Phi_\sigma = A \times (\sigma - \sigma_0)^2 + B \times (\sigma - \sigma_0) + C \quad (\text{Eq 12})$$

where  $A$ ,  $B$  and  $C$  are material constants ( $A$  is  $-3.02 \times 10^{-3}$  1/MPa<sup>2</sup>,  $B$  is  $1.71 \times 10^{-2}$  1/MPa, and  $C$  is  $-2.21$ ).

Therefore, the current creep model of PC is expressed by the master curve of creep compliance (stress shift factor in regime I by Eq 5 and regime II by Eq 12). Regime II (deviation from Eq 5) has not been reported upon in previous studies to our knowledge. As shown in Fig. 4, regime II corresponds to a relatively large stress level, which is close to the yield stress of 66.2 MPa (Ref 27) (a stress difference of 53.8 MPa). We thus hypothesize that this deviation is a breakdown of time–stress superposition principle (TTSP) as described in Eq 5. As mentioned above, this principle assumes that the relationship between the stress-induced increment and the free volume fraction is linear (see Eq 2). However, such a relationship may break down at larger stress levels (such as those close to the yield strength). Indeed, small pores and voids after the yield have been reported by Ikeshima (Ref 31) and others (Ref 32, 33) to nucleate in a polymer material. We thus expected that such nucleation of small voids occurs during creep testing at

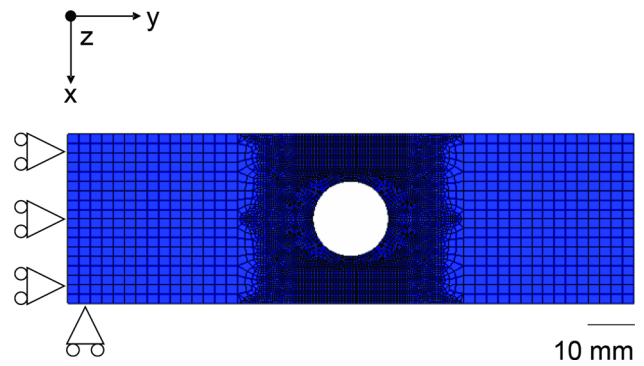


**Fig. 5** Two-dimensional FEM model for PC plate with a circular hole

larger stress levels and longer testing times. This microscopic phenomenon strongly affects Eq 2. Therefore, a new master curve (including Fig. 4) was required for the creep modeling of PC and was established in this study.

#### 4.2 Computational Modeling and Experimental Verifications

To investigate the feasibility of our model, FEM computations and experimental verification were carried out. Since our model can include stress dependency for creep compliance (nonlinear creep), creep deformation for various stress levels must be satisfied. Thus, we used a PC sample with one circular hole exhibiting a gradient stress state in the specimen due to the stress concentration. In order to obtain the local strain around a hole, we used two strain gauges, which were glued 10.5 mm and 15 mm from the center of the circular hole in the experiment.

FEM computation that includes our creep model was carried out in parallel by using the FEM software of Marc Mentat 2012 (MSC Software) (Ref 34). The model is shown in Fig. 5. A two-dimensional model with the plane stress condition was created. The model consists of 9084 meshes with 9335 nodes. In this computation, our model of nonlinear creep (the master curve for the creep compliance and shift factor) was used in the user subroutine (see Marc User Manual (Ref 34)). The Young's modulus for PC was 2.2 GPa (Ref 27) and the Poisson's ratio was 0.37 (Ref 35), as determined in the previous studies. We first conducted an elastic analysis, in which uniaxial loading was applied up to the desired force (750 N), and then the applied load was fixed so that creep analysis could be carried out. We then measured the macroscopic and microscopic deformation behavior experimentally and numerically.

Figure 6 shows the macroscopic creep strain with comparison between experimental and FEM computation results. The macroscopic creep strain was obtained from the measured creep displacement by marker tracking. (Two markers were added 120 mm in length). We found that the FEM data agreed well with the experimental data.

We next investigated the creep deformation in a local area. Figure 7 shows a contour map of the equivalent stress field during the creep test. We found that a remarkable stress gradient develops around the circular hole because of the stress concentration. This indicates that our FEM achieves the development of various stress levels leading to nonlinear creep deformation. In addition, each local stress was almost constant during the creep test. Near the hole, the stress reaches 41 MPa, which is in regime II, as shown in Fig. 4. Figure 8 shows the



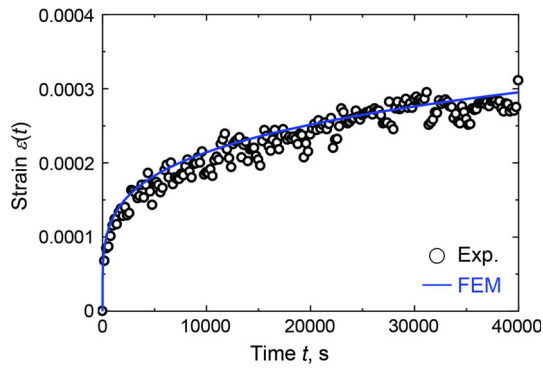


**Fig. 6** Creep strain curves as function of creep time, obtained by FEM computation and experiment. Note that the specimen has one circular hole with a radius of 8 mm (like Fig. 5 of circular hole specimen)

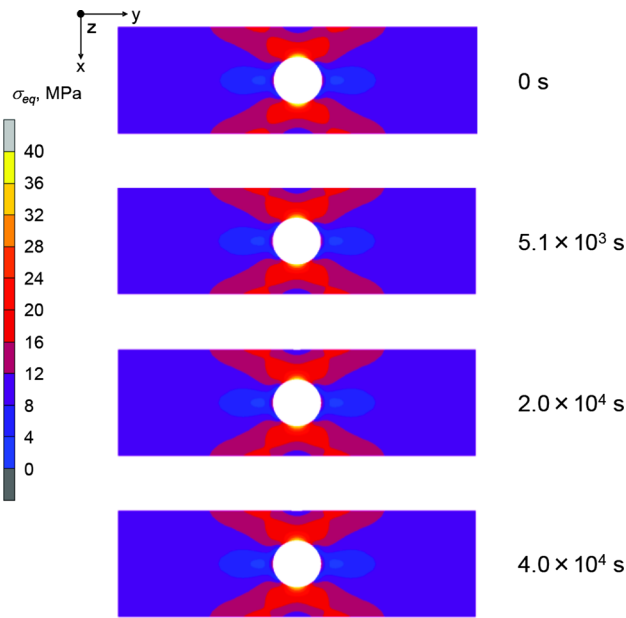


**Fig. 7** Contour map of the equivalent stress field during creep test of the circular hole specimen

contour map of the creep strain field during the creep test. Each snapshot corresponds to each one in Fig. 7. We found that the local creep strain increases with the creep time. As shown in these figures, we found that the creep strain evolved and increased, depending on the local stress level.

To verify our FEM model, we compared the local creep strains obtained by FEM and experiment. Figure 9 shows creep strain curves as a function of creep time at each strain gauge. Here we calculated the difference in between experimental data and FEM computational ones. This shows the maximum deviation at  $r = 10.5$  mm is  $-10.3\%$ , and that at  $r = 15$  mm is  $-2.1\%$ . Therefore, it is concluded that the FEM data relatively agreed with the experimental data at both measurement area. Our creep model can be applied to a sample having a remarkable stress gradient leading to nonlinear creep deformation. Therefore, our model can cover a wide range of larger applied stresses for which general TTSSP cannot be valid.

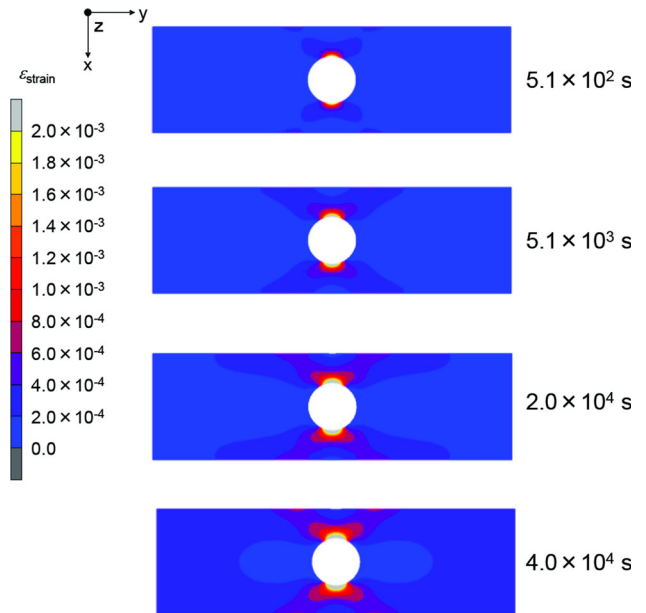


**Fig. 8** Contour map of the creep strain field during creep test of the circular hole specimen

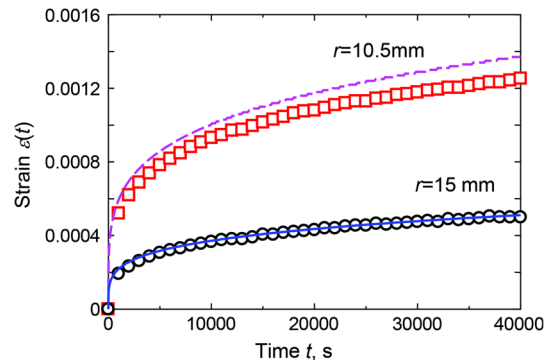


**Fig. 9** Creep strain curves as function of creep time for local measurement area from experiment (open marks) and FEM computation (lines) for the circular hole specimen. The measurement area (radius from the center) is also shown

## 5. Conclusion

This study established a numerical model for the nonlinear creep deformation of PC. This model can predict a creep compliance curve for a wide range of applied stress levels. First, uniaxial tensile creep tests were conducted at eight different stress levels to investigate the effect of applied stress on creep compliance (i.e., nonlinear creep deformation behavior). Next, TTSSP was used to obtain the master curve for creep compliance. TTSSP was previously established on the basis of free volume theory with respect to stress level. When we appropriately selected the stress reduced time, we obtained the master curve, which unifies the creep compliance curves for any stress level. However, we found that the stress shift factor is not expressed by TTSSP, in particular the large stress level deviates from the equation of a previous TTSSP. This may be due to nucleation of small voids during creep testing at larger stress levels, resulting in the unsuitability of the free volume

theory for an actual creep model. Thus, this study modified the stress shift factor to establish a master curve, which was introduced to FEM for numerical modeling. To verify our model, we conducted tension creep tests on a circular hole sample, the tensile stress of which is developed with a gradient because of the stress concentration near the hole. For the macroscopic creep strain and local creep strain near the hole, we found that the FEM data agreed well with the experimental data. Therefore, our model may be useful for the nonlinear creep deformation of PC, which may cover a wide range of applied stress levels.

## Acknowledgments

This work is supported by the JSPS KAKENHI (Grant No. 17K06062) from the Japan Society for the Promotion of Science (JSPS) and by a research grant from the Suga Weathering Technology Foundation (SWTF) (No. 67).

## References

- Z.N. Yin and T.J. Wang, Deformation Response and Constitutive Modeling of PC, ABS and PC/ABS Alloys Under Impact Tensile Loading, *Mater. Sci. Eng., A*, 2010, **527**, p 1461–1468
- K. Cao, X. Ma, B. Zhang et al., Tensile Behavior of Polycarbonate Over a Wide Range of Strain Rates, *Mater. Sci. Eng., A*, 2010, **527**, p 4056–4061
- M. Ito, Y. Masuda, and K. Nagai, Evaluation of Long-Term Stability and Degradation on Polycarbonate Based Plastic Glass, *J. Polym. Eng.*, 2014, **35**, p 31–40
- T. Sakai and S. Somiya, Analysis of Creep Behavior in Thermoplastics Based on Visco-Elastic Theory, *Mech. Time-Depend. Mater.*, 2011, **15**, p 293–308
- M.L. Williams, R.F. Landel, and J.D. Ferry, The Temperature Dependence of Relaxation Mechanisms in Amorphous Polymers and Other Glass-forming Liquids, *J. Am. Chem. Soc.*, 1955, **77**, p 3701–3707
- T. An, R. Selvaraj, S. Hong, and N. Kim, Creep Behavior of ABS Polymer in Temperature-Humidity Conditions, *J. Mater. Eng. Perform.*, 2017, **26**, p 2754–2762
- A. Bozorg-Haddad and M. Iskander, Comparison of Accelerated Compressive Creep Behavior of Virgin HDPE Using Thermal and Energy Approaches, *J. Mater. Eng. Perform.*, 2011, **20**, p 1219–1229
- L.C.E. Struik, *Physical aging in amorphous polymers and other materials*, Elsevier, London, 1978
- D. Cangialosi, H. Schut, Veen Av, and S.J. Picken, Positron Annihilation Lifetime Spectroscopy for Measuring Free Volume during Physical Aging of Polycarbonate, *Macromolecules*, 2003, **36**, p 142–147
- B. Xu, Z. Yue, and X. Chen, Analysis of Damage During Bending Creep Tests, *Philos. Mag. Lett.*, 2009, **89**, p 335–347
- W. Luo, C. Wang, R. Zhao et al., Creep Behavior of Poly(Methyl Methacrylate) with Growing Damage, *Mater. Sci. Eng., A*, 2008, **483–484**, p 580–582
- G.U. Losi and W.G. Knauss, Free Volume Theory and Nonlinear Thermoviscoelasticity, *Polym. Eng. Sci.*, 1992, **32**, p 542–557
- W.G. Knauss and I. Emri, Volume Change and Nonlinearly Thermo-Viscoelasticity Constitution of Polymers, *Polym. Eng. Sci.*, 1987, **27**, p 86–100
- P.A.O. Connel and G.B. McKenna, Large Deformation Response of Polycarbonate: Time-Temperature, Time-Aging Time, and Time-Strain Superposition, *Polym. Eng. Sci.*, 1997, **37**, p 1485–1495
- B. Bernstein and A. Shokooh, The Stress Clock Function in Viscoelasticity, *J. Rheol.*, 1980, **24**, p 189–198
- J. Lai and A. Bakker, Analysis of the Non-linear Creep of Highdensity Polyethylene, *Polymer*, 1995, **36**, p 93–99
- W. Luo, T. Yang, and Q. An, Time-Temperature-Stress Equivalence and Its Application to Nonlinear Viscoelastic Materials, *Acta Mech. Solida Sin.*, 2001, **14**, p 195–199
- S. Jazouli, W. Luo, F. Bremand, and T. Vu-Khanh, Application of Time-Stress Equivalence to Nonlinear Creep of Polycarbonate, *Polym. Test.*, 2005, **24**, p 463–467
- J. Kichenin, K.D. Van, and K. Boytard, Finite-Element Simulation of a New Two-Dissipative Mechanisms Model for Bulk Medium-Density Polyethylene, *J. Mater. Sci.*, 1996, **31**, p 1653–1661
- H. Lu, B. Wang, J. Ma et al., Measurement of Creep Compliance of Solid Polymers by Nanoindentation, *Mech. Time Depend. Mater.*, 2003, **7**, p 189–207
- R. Seltzer and Y.-W. Mai, Depth Sensing Indentation of Linear Viscoelastic-Plastic: A Simple Method to Determine Creep Compliance, *Eng. Fract. Mech.*, 2008, **75**, p 4852–4862
- W. Luo, C. Wang, X. Hu, and T. Yang, Long-Term Creep Assessment of Viscoelastic Polymer by Time-Temperature-Stress Superposition, *Acta Mech. Solida Sin.*, 2012, **25**, p 571–578
- R.A. Schapery, On the Characterization of Nonlinear Viscoelastic Materials, *Polym. Eng. Sci.*, 1969, **4**, p 295–310
- S.C. Yen and F.L. Williamson, Accelerated Characterization of Creep Response of an Off-Axis Composite Material, *Compos. Sci. Technol.*, 1990, **38**, p 103–110
- W. Brostow, Time-Stress Correspondence in Viscoelastic Materials: An Equation for the Stress and Temperature Shift Factor, *Mater. Res. Innov.*, 2000, **3**, p 347–351
- W.J. MacKnight and J.J. Aklonis, *Introduction to Polymer Viscoelasticity*, Vol 2, Wiley-Interscience Publication, London, 1983
- N. Inoue, A. Yonezu, Y. Watanabe et al., Prediction of Asymmetric Yield Strengths of Polymeric Materials at Tension and Compression Using Spherical Indentation, *J. Eng. Mater. Technol.*, 2017, **139**, p 0210021–02100211
- H. Zamanian, B. Marzban, P. Bagheri, and M. Gudarzi, On Stress Concentration Factor for Randomly Oriented Discontinuous Fiber Laminas with Circular/Square Hole, *J. Sci. Eng.*, 2013, **3**, p 7–18
- S.P. Zaoutos, G.C. Papanicolaou, and A.H. Carbon, on the Non-Linear Viscoelastic Behaviour of Polymer-Matrix Composites, *Compos. Sci. Technol.*, 1998, **58**, p 883–889
- A.M. Vinogradov, V.H. Schmidt, G.F. Tuthill, and W.G. Bohannon, Damping and Electromechanical Energy Losses in the Piezoelectric Polymer PVDF, *Mech. Mater.*, 2004, **36**, p 1007–1016
- D. Ikeshima, A. Yonezu, and L. Liu, Molecular Origins of Elastoplastic Behavior of Polycarbonate Under Tension: A Coarse-Grained Molecular Dynamics Approach, *Comput. Mater. Sci.*, 2018, **145**, p 306–319
- Y. Higuchi and M. Kubo, Coarse-Grained Molecular Dynamics Simulation of the Void Growth Process in the Block Structure of Semicrystalline Polymers, *Modell. Simul. Mater. Sci. Eng.*, 2016, **24**, p 1–13
- K. Hagita, H. Morita, and H. Takano, Molecular Dynamics Simulation Study of a Fracture of Filler-Filled Polymer Nanocomposites, *Polymer*, 2016, **99**, p 368–375
- MSCsoftware. Marc® 2012 Volume D: User Subroutines and Special Routines
- M. Fukuhara and A. Sampei, Low-Temperature Elastic Moduli and Dilational and Shear Internal Friction of Polycarbonate, *Jpn. J. Appl. Phys.*, 1996, **35**, p 3218–3221

**Publisher's Note** Springer Nature remains neutral with regard to jurisdictional claims in published maps and institutional affiliations.